Magnetic energy loss in permalloy thin films and microstructures

Corneliu Nistor,* Eshel Faraggi,† and J. L. Erskine
Physics Department, The University of Texas at Austin, Austin, Texas 78712, USA
(Received 11 June 2004; revised manuscript received 20 April 2005; published 1 July 2005)

Magnetic switching and energy loss scaling is studied in permalloy thin films and microstructures over a nine-decade frequency range. The dynamic coercive field $H_c^*(\omega)$ of both the films and the microstructures can be accurately described by a three-parameter scaling function $H_c^*(\omega)=H_{dp}+K(dH/dt)^\alpha$ derived from a domain-wall dynamics model driven by a linear ramp field. The scaling function describes frequency-dependent evolution from adiabatic to domain-wall dominated power-law loss behavior without invoking mechanism crossover (to nucleation-dominated behavior) and manifests scaling exponents that depend only weakly on static coercivity. High-quality thin-film microstructures produced by vacuum evaporation yield $\alpha=1/2$, a universal exponent associated with domain-wall dominated magnetization reversal based on a linear-mobility model. Corresponding films and microstructures prepared by sputtering also exhibit power-law scaling based on a smaller α, but still consistent with domain-wall rather than nucleation-based reversal. The results suggest that in the thin-film limit large-angle local spin damping mechanisms account for magnetic energy loss at both low frequencies (Barkhausen regime in which pinning dominates average domain-wall velocity) and high frequencies (power-law scaling regime in which the mobility dominates average domain-wall velocity).

DOI: 10.1103/PhysRevB.72.014404 PACS number(s): 75.40.Gb, 75.60.Ej, 75.70.Ak

I. INTRODUCTION

Magnetization reversal in ferromagnetic materials is accompanied by energy dissipation that can be characterized by hysteresis loop measurements. The loop area of the magnetization versus applied magnetic field intensity curve $M(H)$ equals the magnetic energy loss per cycle. Intrinsic magnetic (hysteresis) energy dissipation occurs at the lowest frequencies experimentally attainable; it results from irreversible, discontinuous, and generally small changes in magnetization known as Barkhausen jumps.[1] Single-sweep $M(H)$ loop measurements of small magnetic samples reveal that hysteresis loss exhibits statistical behavior: loop shapes, loop areas, and dynamic coercivity H_c^* defined by $M(H_c^*)=0$ vary from cycle to cycle and depend on sweep rate. Multiple-cycle averaging leads to stable values for loop area $A(H_0,\omega)$ and dynamic coercivity $H_c^*(H_0,\omega)$, which are functions of the drive-field amplitude H_0 and frequency ω. Early work by C. P. Steinmetz and Rayleigh[1] established empirical power laws that describe magnetic energy loss scaling for laminated magnetic material over a limited range of drive field parameters.

In addition to intrinsic magnetic energy losses, magnetic metals exhibit classical eddy-current losses which scale as $\omega^2 B_0^2 \Delta x\, \sigma$, where B_0 is the maximum value of magnetic induction and Δx and σ characterize the material thickness and conductivity, respectively. In very thin films ($\Delta x \to 0$) classical (nonlocal) eddy-current losses become negligible compared to intrinsic losses associated with domain-wall (DW) damping effects, thus permitting measurement of intrinsic magnetic loss scaling. Microscopic models of DW dynamics in magnetic insulators and metals have established relationships between the applied magnetic field and generalized wall motion through effective wall forces, masses, and energies.[2] In insulating materials the energy loss is introduced through (local) gyromagnetic effects (damping term in the Landau-Lifshitz-Gilbert equation); in metals, wall-motion driven eddy-current effects can limit DW mobility, but these effects manifest the same scaling as classic eddy-current loss: the eddy-current wall damping losses scale as Δx and the wall mobility scales as Δx^{-1}. For thin ($\Delta x < 1000$ Å) and ultrathin ($\Delta x < 10$ Å) films, eddy-current wall-damping loss becomes negligible and the wall mobility presumably is limited by gyromagnetic damping, as in insulating materials. Therefore one important feature of magnetization dynamics in two-dimensional systems (thin and ultrathin films) is the high DW mobility.

Analysis of the energy loss in a driven magnetic system as a function of H_0 and ω (and temperature T), in principle, offers access to the physical processes that govern magnetic hysteresis and switching through analysis of hysteresis loop shape and energy loss scaling behavior. Surprisingly, there have been no conclusive systematic investigations of energy loss scaling in magnetic materials that have resulted in experimentally verified realistic general models that connect measured hysteresis loss scaling with intrinsic loss mechanisms.[3–14]. Recent theoretical studies[3,11–14] have explored magnetic hysteresis energy loss in various model magnetic systems based on phenomenological approaches and numerical simulations. One objective of these studies was to test concepts of universality and scaling in dynamical systems. Many of the model systems studied were found to yield power-law scaling behavior for the magnetic energy loss per cycle in terms of H_0, ω, and T of the form

$$A \propto H_0^\alpha \omega^\beta T^{-\gamma}, \tag{1}$$

where α, β, and γ are universal exponents that depend on the dimensionality and the symmetries of the system. Analytical models and numerical simulations based on nucleation processes[12–14] yield logarithmic rather than power-law scaling.

Experimental studies of magnetic hysteresis in thin and ultrathin films[4–10] and microstructures[11] have also explored the dynamics of magnetization reversal and probed for evidence of universal scaling. While there have been claims of experimental observation of universal scaling behavior,[4,5,9,10] the existence of universal dynamic exponents remains controversial; this and other assertions based on interpretation of experimental results remain to be verified or refuted. Selected disturbing discrepancies include: (1) incompatibility of experimental data for ultrathin film dynamic scaling exponents and various theoretical models (tables in Refs. 6–8 and 11); (2) inconsistencies in claims of observing single exponent scaling, $A \propto (dH/dt)^{\alpha}$,[9,10] i.e., $\alpha=\beta$; (3) assertions that crossover from adiabatic (very small β) to more rapid (larger β) energy loss scaling observed in some systems results from a change of reversal mechanisms from DW motion to nucleation.[8,9,13] From these results and the discussion which follows, it is clear that prior attempts to connect measurements of energy loss scaling with theoretical models have had limited if any success.

In this paper we address these issues, successfully identify the origin of some of the inconsistencies, and resolve them. We demonstrate that the energy loss scaling of permalloy films and microstructures fabricated from the same films can be accurately described over a broad frequency range by a scaling function of the form[7]

$$A = A_0 + K\left(\frac{dH}{dt}\right)^{\alpha}, \tag{2}$$

where the constants A_0, K, and α are later shown to be related to the following parameters in a domain dynamics model: H_{dp}, the depinning field; μ, the DW mobility; ρ, the nucleation density or spatial scaling factor; and α, an exponent that enters the expression for the DW velocity as a function of the applied field. Our simple DW model derivation of the scaling function, Eq. (2), and the parametrization of the model are compatible with a more sophisticated comprehensive treatment of hysteresis behavior reported by Lyuksyutov *et al.*[14] Curve fitting of experimental data for large area films and microstructures *fabricated from the same sample* covering over an eight decade frequency range yield excellent fits with different values of A_0 (static coercivity), but nearly identical values of α, suggesting that the scaling function [Eq. (2)] is universal and that the exponent α that governs the loss scaling is essentially independent of sample size or shape. The result $\alpha=1/2$ for microstructures fabricated from high-quality vacuum-deposited permalloy films on Si could be an indication that these films satisfy the conditions required[14] to achieve universal scaling resulting from DW motion of a rigid wall in a system characterized by weak disorder. These results clarify several issues pertaining to hysteresis loss scaling and along with our simple model and more detailed models[14] provide a framework for interpreting hysteresis loop shapes and loss scaling measurements in terms of parameters that appear in the conventional description of DW dynamics.

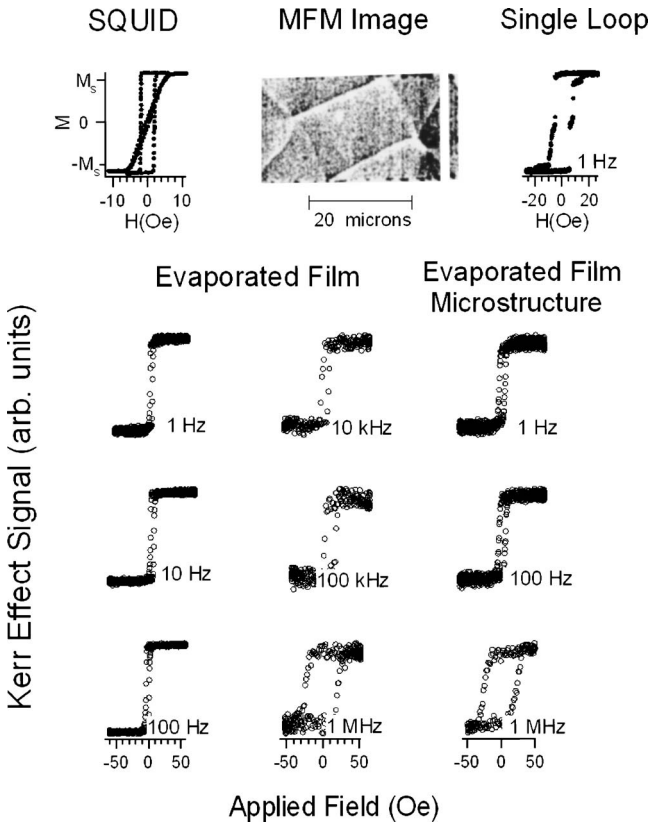

FIG. 1. Representative hysteresis loops for permalloy film structures. SQUID loop displays easy- and hard-axis magnetization of the 30 nm thick sputtered sample. The MFM image displays a remanent domain pattern of a 30 nm thick evaporated film microstructure. Single-loop scan of an evaporated film microstructure shows Barkhausen jumps. All other loops, representing multiple-sweep averages, measured at various frequencies show the variation of H_c^* as the drive frequency is changed. Drive-field amplitude for all loss scaling measurements was maintained at approximately 50 Oe. Each loop contains 300 points and the temporal resolution exceeds the sampling time between points by a factor of 10 or more at all frequencies.

II. EXPERIMENT

Two types of permalloy ($Ni_{80}Fe_{20}$) thin-film samples were studied: samples prepared by sputtering and by vacuum evaporation. In both cases, microstructures as well as large-area (millimeter scale) samples were prepared from the same parent films. All films were prepared on high-quality commercially polished Si(100)$\pm$0.5° wafers. The sputtered permalloy film sample was a multilayer stack 5 nm Ta/30 nm permalloy/5 nm Ta grown on a Si(100) surface with a 10 nm SiO_2 coating. Superconducting quantum interference device (SQUID) magnetometry verified an easy-axis direction with $H_c \approx 2$ Oe and a hard-axis direction with M_s occurring at an applied field of 6 Oe (Fig. 1). Low drive-frequency hysteresis loops measured by magneto-optic Kerr effect (MOKE) polarimetry reproduced the SQUID results. Microstructures (produced by electron-beam lithography and etching) of the same sputtered-film sample yielded loops exhibiting Barkhausen jumps and average values of low-frequency co-

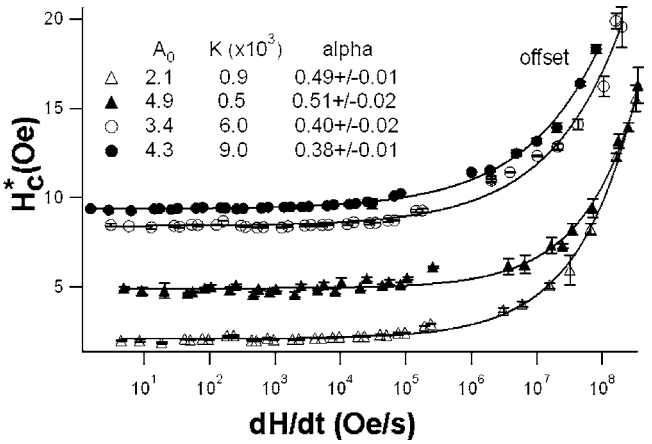

FIG. 2. Variation of H_c^* as a function of dH/dt for four permalloy samples: circles, sputtered film microstructures (20×40 microns full circles), and large parent film (2 mm$\times$2 mm open circles); and triangles, evaporated film microstructures from the same parent film (50×50 microns full triangles, 100×150 microns open triangles). The figure gives values for the parameters in Eq. (2) that produce best fits represented by solid lines. Note that A_0 is essentially the static coercivity (upper two curves offset by 5 Oe for clear presentation).

ercive fields that were higher than that of the larger samples of the same film (Figs. 1 and 2). The vacuum-evaporated films were prepared in UHV by electron-beam evaporation from a tungsten molecular beam epitaxy (MBE) cell and microstructures were fabricated by standard lift-off techniques. Auger electron spectroscopy confirmed the stoichiometry and atomic force microscopy confirmed thickness calibrations. The 30 nm sputtered films/microstructures and the corresponding evaporated films/microstructures exhibit very similar high-frequency scaling behavior, but significantly different static coercivities (Fig. 2).

Magnetic switching transients and hysteresis loops were measured by a high-speed high-spatial-resolution MOKE polarimeter incorporated into a long-focal-length polarized-light microscope.[15] Recent upgrades of the optics, drive-field amplifiers, impedance matching devices, detectors, and detection instruments now permit spatially resolved (1 μm) measurements of magnetization at 1 ns time resolution using continuous-wave drive-field amplitudes of approximately 100 Oe and frequencies from below 0.001 Hz to above 50 MHz. The magnetic field required to drive the sample is produced by either a half-centimeter long No. 20 Cu wire soldered between thick Cu electrodes, or by Helmholtz coils approximately 1 cm in diameter; both produce fields of approximately 5 Oe/amp. The current generating the driving magnetic field was measured over overlapping operating ranges by various devices including a noninductive resistor (dc—10 KHz), active current transducer, Danfysik 860R (dc—500 KHz), LeCroy 50 MHz current probe, and Pearson current transformers (No. 2870/70 MHz; and No. 2877/200 MHz). $M(t)$ and $H(t)$ wave forms were measured and signal averaged by a digital oscilloscope (LeCroy 960). The 3 dB bandwidth of the $H(t)$ channel (200 MHz) and $M(t)$ channel (>300 MHz) were sufficiently wide to yield approximately a 1 ns time resolution. Relative phase shifts of the $H(t)$ and $M(t)$ channels were negligible below 10 kHz; measured values of H_c^* at higher frequencies were corrected ($\sim$20% at highest frequency) based on phase-shift calibrations.

III. RESULTS

Figure 1 displays representative multiple-cycle average easy-axis hysteresis loops for the evaporated and sputtered permalloy films and microstructures; each loop contains approximately 300 points. The variation of $H_c^*(\omega)$ can be seen as the increase in the width of the loops.

Loops were measured using both sine and sawtooth (piece-wise linear ramp) wave forms. Both wave forms produced identical hysteresis loops and energy loss scaling that depend only on dH/dt, provided $H_0 \gg H_c^*$. This condition ensures that for the sine wave form $\frac{dH}{dt}(H=H_c^*) \approx \frac{dH}{dt}(H=0) = H_0\omega$, hence the sinusoidal wave-form problem can be reduced to the corresponding piece-wise linear problem. In this case, *the scaling can only depend on* dH/dt and $\alpha \equiv \beta$ if Eq. (1) scaling is applied. We note that this condition is invoked in Ref. 14 to obtain $\sqrt{\omega}$ scaling based on sine-wave drive-field excitation.

Figure 2 displays the scaling of H_c^* as a function of dH/dt for four permalloy samples. All loops used to plot the points in Fig. 2 were driven beyond saturation as previously described and shown in Fig. 1 and were averaged over many cycles. The large area films and the fabricated microstructures exhibit similar scaling of H_c^*: an adiabatic region of low frequencies (small increase of H_c^*) followed by a transition to a region of more rapidly increasing energy loss.

It is clear that the scaling law Eq. (1) is incapable of fitting the experimental results over the entire frequency range, although "effective" exponents[5,9,10] can be obtained by fitting one or two decades. On the other hand, excellent fits using the scaling function Eq. (2) are shown in Fig. 2. In this case A_0, representing the quasistatic coercivity, is significantly different for the films and microstructures but common exponents are obtained from the fit for samples obtained from each parent film.

IV. SCALING LAW

The scaling law, Eq. (2), can be obtained as an exact solution of an extension of the domain dynamics model first described by Williams, Shockley, and Kittel[16] in relation to studies of domain propagation velocities. The model describes a linear relationship between the DW velocity v and the applied field, $H > H_{dp}$ in terms of a mobility parameter μ and the depinning field H_{dp}: $v=\mu(H-H_{dp})$. DW velocity measurements based on a (bulk) SiFe single crystal picture frame sample were used to show that eddy-current damping accounted for the mobility μ. The scaling law derivation we present is highly simplified (but perhaps more transparent) compared to the rigorous analysis reported by Lyuksyutov *et al.*[14] and follows a corresponding simplified model reported by Ruiz-Feal *et al.*[17] which is based on the assumption of a sinusoidal drive field and a linear mobility model. Our as-

sumption of linear ramp drive field simplifies integrations and the nonlinear form of the mobility equation, which is often employed in detailed treatments of DW motion,[14,18] leads to a simple algebraic relationship between the exponents q [Eq. (3)] and α [Eq. (2)]. We note here, and discuss later, that setting $q=1$ in Eq. (3) leads to $\alpha=1/2$ in Eq. (2) in our model, as well as in the model of Lyuksyutov *et al.*[14] The expression for the DW velocity $v(H)$ in terms of its mobility μ and the depinning field that includes an exponent q is assumed to be

$$v(H)=\begin{cases}0 & H<H_{\mathrm{dp}}\\ \mu(H-H_{\mathrm{dp}})^q & H\geqslant H_{\mathrm{dp}},\quad q>0.\end{cases} \tag{3}$$

We further assume that the applied field is a piece-wise linear ramp function of time

$$H(t)=-H_0+h_0t. \tag{4}$$

The linear (rather than sinusoidal) form of $H(t)$ is compatible with the experimental conditions achieved in our measurements and also allows analytical expressions for $H_c^*(\omega)$ to be obtained from the one-dimensional, two-dimensional, and field-dependent nucleation models treated by Ruiz-Feal *et al.*[17]

The expression for dynamic coercivity in a model consisting of circular domains of radius r and density ρ is obtained in the following manner. The differential area element covered by a wall displacement dr is $2\pi\rho r dr$ and the resulting change in normalized magnetization is

$$dm=4\pi\rho r dr. \tag{5}$$

If the density of nucleating reversed domains is designated by ρ, the average distance a DW covers in two dimensions is $r_s=1/\sqrt{\rho}$ which will be referred to as the saturation length. Saturation is incorporated into the model by introducing $dm\propto\rho r(r_s-r)$, where from the saturation condition $2=\int_{-1}^{1}dm$ the proportionality constant is found to be $12/r_s$, and

$$dm=12\rho^{-3/2}r(r_s-r)dr. \tag{6}$$

The magnetization is obtained by integrating Eq. (6)

$$m(r)=-1+2\rho^{3/2}r^2(3r_s-2r), \tag{7}$$

where r(H) is obtained from the velocity of the DW Eq. (3), with $H(t)$ defined by Eq. (4). Integrating this last expression we obtain from Eq. (4) $dH=h_0dt$, and $dr=vdt=v(H)dH/h_0$

$$r(H)=\begin{cases}0 & H<H_{\mathrm{dp}}\\ \frac{\mu}{(q+1)h_0}(H-H_{\mathrm{dp}})^{q+1} & H\geqslant H_{\mathrm{dp}},\quad q>0\\ r_s & H>H_s.\end{cases} \tag{8}$$

With H_s obtained from the condition $r_s=r(H_s)$

$$H_s=H_{\mathrm{dp}}+\sqrt[q+1]{\frac{(q+1)h_0}{\mu\sqrt{\rho}}}. \tag{9}$$

The dynamic coercive field H_c^* is found from the condition of zero magnetization $m(H_c^*)=0$. An expression for this condition is obtained by considering the coercive radius r_c, the distance a DW would have to sweep for the magnetization to reach zero, i.e., $m(r_c)=0$. This condition yields

$$1=\int_0^{r_c}12\rho^{-3/2}r(r_s-r)dr, \tag{10}$$

which results in

$$1=\frac{2}{r_s^3}(3r_sr_c^2-2r_c^3). \tag{11}$$

For $r_c\in[0,r_s]$ Eq. (11) has a single solution, $r_c=r_s/2$. Therefore, an implicit condition for the dynamic coercive field in this model becomes

$$\frac{h_0r_s}{2}=\int_{-H_0}^{H_c^*}v(H)dH. \tag{12}$$

After performing the integration, the dynamic coercive field for this case is found to be

$$H_c^*=H_{\mathrm{dp}}+\sqrt[q+1]{\frac{(q+1)r_sh_0}{2\mu}}=A_0+K(dH/dt)^{\alpha} \tag{13}$$

with

$$\alpha=1/(q+1), \tag{14}$$

and the units of μ are defined by Eq. (3). Thus the expression for DW velocity Eq. (3) plus the assumption of a linear ramp drive field leads directly to the scaling function Eq. (2) with scaling exponent α related to q in Eqs. (3) and (14).

In this model the apparent crossover from adiabatic to frequency-dependent scaling is not necessarily a consequence of mechanism crossover (wall motion to nucleation)[8,13] but can result from the frequency-dependent component of H_c^* competing with the static coercivity. The power-law scaling function Eq. (2) should remain valid as long as the expression for the DW velocity Eq. (3) remains valid. At this point it is informative to again note that models that emphasize nucleation[12] or in which nucleation dominates the dynamics[12–14] predict scaling functions that are logarithmic.

V. ADIABATIC LIMIT

Magnetic energy loss in our permalloy samples at low frequencies is independent of drive-field frequency (Fig. 2, $dH/dt<10^4$ Oe/s) but clearly depends on sample geometry and growth technique: Samples having different geometries fabricated from the same parent film exhibit the same value for α (within experimental error) but manifest significantly different values of A_0 (the average static coercivity). The geometry-dependent variation of A_0 is expected, based on demagnetizing factors (shape anisotropy). The table (Fig. 2) also suggests α is sensitive to the (growth-dependent) film microstructure, but addressing this feature of our results lies beyond the scope of the present paper. In this section, we briefly examine the absence of frequency-dependent scaling at low drive frequencies and the crossover to a different dynamic regime characterized by a rapid increase of magnetic

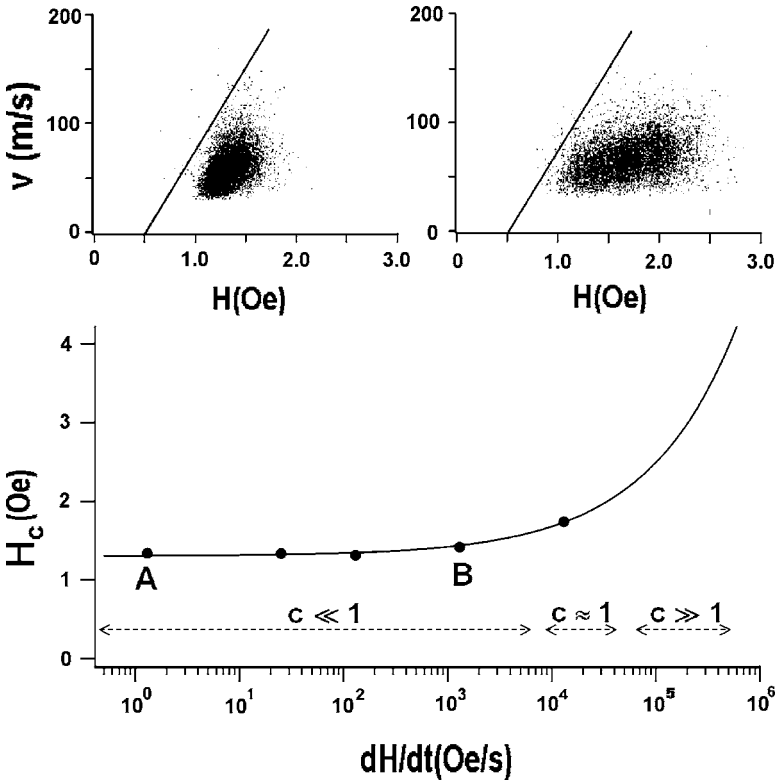

FIG. 3. Scaling function (solid curve) and BJ velocity distributions adapted from Ref. 19. The solid circles A and B plotted on the curve represent distribution averages; they correspond respectively to the left and the right insets.

energy loss with increasing dH/dt. A more extensive account of the Barkhausen phenomena that dominate the DW dynamics at low drive-field sweep rates is presented in a separate publication.[19] In the low-frequency limit, Eq. (3) is valid only in the sense that multiple-cycle averages over sufficiently large volumes are needed to define meaningful values for the average DW velocity v, average mobility μ, and average depinning field H_{dp}. At low sweep rates (adiabatic limit) it is possible to measure (using the same methodology described in the experimental section) the random changes in magnetization known as Barkhausen jumps (refer to single loop displayed in Fig. 1). In this limit, the domain dynamics description Eq. (3) can be generalized by postulating that the instantaneous local wall velocity is governed by[20,21]

$$v = \mu'[H - (H_{\mathrm{dm}} + H_p)], \tag{15}$$

where the constant geometry-dependent demagnetizing field H_{dm} is separated from a random component H_p that includes all local (short-range) counterfield contributions. The mobility parameter μ' can be viewed as a statistical parameter with a maximum value μ'_{max} governed by a suitable wall-damping mechanism. In bulk samples, μ'_{max} is governed by eddy-current wall damping described by Williams *et al.*[16] In thin films, our experiments[19] have demonstrated that μ'_{max} is governed by the local spin-damping parameter α_G that appears in the Landau-Lifshitz-Gilbert equation. The pinning field H_p is assumed to be a Brownian function of the local DW position. The DW motion resulting from a linear-ramp applied field $dH/dt \propto c$ can be obtained analytically[22] from Eq. (15) yielding among other predictions scaling functions[22–24] that govern the distribution of DW velocities (v), Barkhausen jump amplitudes (ΔM), and jump times ($\Delta\tau$)

$$P(v) = v^{-\alpha'} f(v/v_0), \quad \alpha' = 1 - c, \tag{16}$$

$$P(\Delta M) = (\Delta M)^{-\beta} f(\Delta M/\Delta M_0), \quad \beta = 3/2 - c/2, \tag{17}$$

$$P(\Delta\tau) = (\Delta\tau)^{-\gamma} f(\Delta\tau/\Delta\tau_0), \quad \gamma = 2 - c, \tag{18}$$

where $c \propto dH/dt$ is a dimensionless parameter that characterizes the sweep rate, and $f()$ is a cutoff function. Barkhausen phenomena including the scaling relationships have been studied extensively[18,20–23] (and verified) in bulk systems where μ' is governed by eddy-current damping. For example, experiments at low sweep rates ($c \to 0$) on systems having an upper critical dimension $d=3$ obtain $\beta=3/2$. Higher sweep rates lead to the condition $c \approx 1$ which corresponds to a crossover regime in which the DW motion is no longer assumed to be characterized by intermittent jumps described by the distribution functions Eqs. (16)–(18) and by Eq. (15). At sufficiently high sweep rates, the DW does not become pinned locally; instead it experiences an average depinning force [H_{dp} of Eq. (3)] and assumes an average velocity v governed by an average mobility. We demonstrate that the crossover from the adiabatic region to the scaling region can be viewed in terms of these two wall-dynamics regimes: $c \ll 1$ (adiabatic) and $c \approx 1$ (onset of scaling). We note that this transition does not necessarily require transformation to nucleation-based reversal mechanism.

Figure 3 displays a graph of $H_c^*(\omega)$ for a 100×150 μm permalloy sample (fitting parameters from Fig. 2) with five points (two of which are labeled A and B) plotted on the

graph. The inset labeled A and B displays values of several thousand measurements of the velocities of individual Barkhausen jumps as a function of the applied field value at which the jump ocurred. Each scatter plot can be viewed as a graphical representation of Eq. (15). The sloping line in each graph represents $\mu'_{\max}$, the maximum mobility which is estimated to be 150 m/s Oe and shown to be compatible with estimates based on local (gyromagnetic) damping. The intercept of this line at $v=0$ is 0.5 Oe corresponding to H_{dm} and the range of H values over which Barkhausen jumps are observed characterizes the range of local variations in H_p.

The value of H_c^* plotted at A and at B represent the average value of the switching field distributions in each graph. The distributions for the two points between A and B are nearly identical to that of A.[19] The significant change in distribution manifested in the scatter plot B corresponds to the transition from $c \ll 1$ to $c \approx 1$, as shown in the figure. The value of the parameter c was accurately estimated from measured values of β, Eq. (17) at several values of dH/dt by plotting $P(\Delta M)$ distributions. Thus Fig. 3 establishes the relationship between the onset of scaling with the transition from the stochastic (Barkhausen) regime to a continuous motion regime. The maximum mobility limit is compatible with the theoretical limit $\mu'_{\max} = \gamma\Delta_0/\alpha$ based on measured parameters for the gyromagnetic constant γ and damping parameter α for permalloy and on a reasonable assumption for the DW width $\Delta \approx 48$ nm.[19] This result shows that local damping governs magnetic loss in the adiabatic region. Mobility measurements at high sweep rates on our films and by others yield values of μ, Eq. (3), of about 150 m/s Oe, which also suggest that local damping governs wall dynamics in this regime.

The Barkhausen jump results provide an intuitive understanding of the adiabatic limit. The magnetic loss remains constant independent of sweep rate because the time scale for completion of a Barkhausen jump is short compared with the sweep-rate period; the jump distributions are therefore independent of dH/dt in this ($c \ll 1$) limit.

The high-frequency limit is dominated by a power-law exponent $\alpha = 1/(1+q)$ which is related to the expression for DW velocity. The power-law scaling function [Eq. (2)] should remain valid as long as the model [Eq. (3)] describes the wall dynamics. The scaling parameters that yield the model fit are presented in Fig. 2.

VI. DISCUSSION

These results clarify some of the confusion surrounding prior measurements of hysteresis energy-loss scaling and interpretation based on various models. Hysteresis loss measurements over a wide frequency range are helpful in revealing the nature of the scaling behavior. The role of the static coercive fields in affecting measured scaling behavior is also revealed by wide frequency range measurements of identical thin-film structures having different two-dimensional geometry (and hence different static H_c values). Magnetic force microscopy (MFM) images of domain pattern and single-loop hysteresis measurements that manifest Barkhausen jumps (Fig. 1 and Ref. 19) provide unambiguous evidence that the energy loss mechanism in the "adiabatic" (<100 Hz) region results from intrinsic wall-damping mechanisms. Nucleation effects account for reconfiguring spins into DWs after the magnetic films recover from being driven to saturation. However, the sweep-rate dependent nucleation magnetic energy loss is apparently very small compared to the loss associated with DW motion during magnetization reversal. Our experiments detect no significant logarithmic scaling, which is a manifestation of nucleation-dominated magnetic energy loss. Restricting drive-field characteristics to linear ramp conditions ($H_0 \gg H_c^*$ for sinusoidal drive fields) ensures dH/dt scaling based on very general arguments.

The previously noted discrepancies in values of α and β resulting from application of Eq. (1) scaling to experimental results can also be understood as follows. Effective exponents obtained by fitting (for example) a two decade range of $H_c^*(\omega)$ can yield any value of β, from very low values associated with Barkhausen-jump based DW motion (adiabatic region) to the larger value obtained at the high frequencies, where power-law scaling occurs ($c \approx 1$ region). Note that the effective β at all but the highest drive frequencies will depend on the specific value of dH/dt where β is calculated, as well as A_0, which is a function of sample thickness, size, shape, and quality. It is also possible to conclude that $\alpha \neq \beta$ by curve fitting experimental results over an inadequate range of drive-field amplitude and/or frequency, or under inequivalent drive field conditions.

We conclude our discussion by establishing a connection between our measurements of hysteresis loss scaling and microwave measurements of the complex permeability spectra of thin permalloy films. In microwave loss experiments the drive-field amplitude is small in relation to the demagnetizing field and the magnetic response involves driven spin precession around M at the drive frequency. In this case (small angle magnetization dynamics) dM/dt follows dH/dt. In these "small-angle" loss measurements the magnetic loss is manifested as an increase in the real part of the complex permeability constant, and a rapid increase in loss scaling is not observed until the drive frequency is high (several hundred MHz). In our experiments the magnetization is driven to saturation $\pm M_s$ during each cycle. At any location in the sample where the loss occurs within a DW the change in magnetization can be written $dM/dt = (dM/dx) \times (dx/dt)$, where dM/dx is approximately the change in $M = 2M_s$ divided by the DW width (Neel wall of order 500 Å) and dx/dt = wall velocity (large-angle magnetization dynamics). An approximate value for DW velocity from the switching time of a microstructure requires knowledge of the number of moving domains. From the 1 MHz loops $\tau_s \approx 0.1$ μs, and if we assume five domains nucleate across 20 μm, the wall velocity is of the order of $1/5 * 20$ μm/0.1 μs ≈ 40 m/s. The switching time for magnetization reversal within the domain is therefore $\tau_M \approx (40\ \mathrm{m/sec})/500$ Å. The corresponding frequency is about 1 GHz [zero field ferromagnetic resonance (FMR) frequency for permalloy films is approximately 500 MHz]. The frequency-dependent loss $\mu''(f)$ for permalloy films[25] in the 40-400 MHz range can be fit by Eq. (2) with $\alpha \approx 0.7$. There is no reason to expect that the scaling

exponents measured in the "small angle" FMR regime and the "large angle" switching regime[26] should be equivalent, but the crossover from adiabatic to higher loss scaling in about the same frequency range suggests that our measurements probe the intrinsic damping magnetic loss at effective drive frequencies approaching 1 GHz.

VII. CONCLUSIONS

This paper has focused exclusively on the room-temperature scaling behavior of hysteresis loss in thin-film permalloy samples. Very encouraging agreement between the experimental results and the loss scaling predicted by a general model describing rectilinear DW motion in a system of weak disorder has been obtained. Important opportunities remain to be explored. The general formulation of DW motion in a random medium[14] has shown that the hysteresis can be characterized by two dynamic threshold fields, the coercive fields H_c^* and the reversal field H_r^*, and that the ratios of this field to the static threshold field H_{dp} can be represented as functions of two dimensionless variables that incorporate material parameters and drive-field parameters(i.e., μ, r_s, $h_0 = H_0\omega$ in our model). We have only explored H_c^*. However, the loops can be time averaged to high precision, and additional dynamic parameters including H_r^* can be measured. Detailed tests of the model should be possible based on loop-shape measurements; in addition, an explicit relationship between parameters describing the loop shape and the mobility function has been derived[14] and can be used to reconstruct the mobility equation from loop-shape measurements.

The idea of examining various sizes and shapes of microstructures fabricated from the same parent film has proven to be very useful in separating the adiabatic term (static coercivity) from the dynamic component of $H_c^*(\omega)$. The adiabatic range for our permalloy films and microstructures extends from the lowest drive frequencies that are practically accessible (0.01 Hz) through 100 Hz, and frequencies extending to 10^7 Hz (nine decades) at drive field amplitudes of 50 Oe were useful in accurately characterizing the scaling. We believe that the results reported in this paper represent unambiguous determination of power-law scaling with $\alpha = 1/2$, which is characteristic of DW motion characterized by a linear mobility function. This result also allows attributing the crossover from the adiabatic magnetic energy loss to $\sqrt{\omega}$ scaling as a simple consequence of the crossover from the Barkhausen effect dominated DW motion (no scaling) to a driven DW motion regime in which the frequency-dependent loss emerges from driven wall dynamics. An equivalent way to correctly view the crossover is that it represents a transition from pinning-dominated to mobility-dominated average DW velocity.

Many features of magnetization reversal dynamics predicted by phenomenological models and numerical simulations remain to be explored and tested based on experiments. Hysteresis loss scaling of the form $A = A_0 + k\omega^{\alpha} H_0^{\beta}$ is predicted to occur in certain limits[14] (adiabatic condition prescribed by low drive-field frequencies and amplitudes in relation to characteristic values). Several experiments report such scaling but have not explored the scaling in sufficient detail to determine if the results are consistent with model predictions. Numerical simulations of DW growth and hysteresis behavior have been carried out for ultrathin films (few monolayer thick) based on the two-dimensional Ising model. These numerical simulations find linear dependence of DW velocity on the applied magnetic field over a wide temperature range with or without order. As expected, the loop shapes and energy loss scaling obtained from the simulations are consistent with the phenomenological model predictions based on a linear mobility assumption; specifically $\sqrt{\omega H_c}$ scaling is obtained for nucleation density independent of ω, and $\sqrt{H_0\omega}$ scaling is obtained if nucleation is also independent of H_0. This scaling has not been observed experimentally in ultrathin films. Nucleation-controlled hysteresis occurs when nucleation processes (which tend to be very fast) represent the longest time scale. The hysteresis loops tend to be square, and it will be difficult experimentally to accurately determine loop-shape parameters. However, it will be possible to measure the hysteresis loss scaling, and it has been well established by phenomenological models and numerical simulation that the scaling function is logarithmic. Since thermal activation plays a primary role in nucleation processes, experiments designed to explore nucleation-dominated hysteresis processes and crossover phenomena involving both nucleation and DW motion will require broad temperature range. Very few experiments have provided definitive information about nucleation dominated hysteresis. The inverse-temperature dependence of adiabatic region scaling reported for ultrathin films[6] is consistent with nucleation, however, the frequency and field-amplitude ranges covered are not sufficient to convincingly differentiate between power-law and logarithmic scaling.

ACKNOWLEDGMENTS

We thank Carlos Gutierrez for providing the sputtered film sample, Shuqiang Yang and the "Center for Nano- and Molecular Science and Technology, UT-Austin" for providing evaporated film microstructures, and Alex deLozanne for electron beam lithography fabrication. E.F. would like to thank Linda Reichl for the many discussions and for providing support through the Welch Foundation and the Engineering Research Program of the Office of Basic Energy Sciences at the U.S. Department of Energy, Grant No. DE-FG03-94ER14465. This work was supported by NSF NIRT/DMR-0404252, the R. A. Welch Foundation Grant No. F-1015 and the Texas Coordinating Board ATP-0099.

*Electronic address: nistorc@physics.utexas.edu
†Ilya Prigogine Center for Studies in Statistical Mechanics and Complex Systems. Present address: Physics Department, Florida International University, Miami, Florida 33199; electronic address: faraggi@physics.utexas.edu

[1] Early work on magnetic hysteresis is documented in R. M. Bosworth, *Ferromagnetism* (Van Nostrand, Princeton, 1951).
[2] An overview of recent work on generalized DW dynamics (L. Walker, W. Doring, J. Slonczewski, J. Bishop) is compiled in A. Hubert and R. Schafer, *Magnetic Domains* (Springer, Berlin, 1998).
[3] References to relevant theoretical work on dynamic scaling with summaries of power-law exponent predictions can be found in experimental papers referenced below, Refs. 4–11, also refer to Refs. 12–14.
[4] Y.-L. He and G.-C. Wang, Phys. Rev. Lett. **70**, 2336 (1993).
[5] Q. Jiang, H.-N. Yang, and G.-C. Wang, Phys. Rev. B **52**, 14911 (1995).
[6] J.-S. Suen and J. L. Erskine, Phys. Rev. Lett. **78**, 3567 (1997).
[7] J.-S Suen, M. H. Lee, G. Teeter, and J. L. Erskine, Phys. Rev. B **59**, 4249 (1999).
[8] W. Y. Lee, B.-Ch. Choi, Y. B. Xu, and J. A. C. Bland, Phys. Rev. B **60**, 10216 (1999).
[9] B. C. Choi, W. Y. Lee, A. Samad, and J. A. C. Bland, Phys. Rev. B **60**, 11906 (1999).
[10] W. Y. Lee, B. C. Choi, J. Lee, C. C. Yao, Y. B. Xu, D. G. Hasko, and J. A. C. Bland, Appl. Phys. Lett. **74**, 1609 (1999).
[11] T. A. Moore, J. Rothman, Y. B. Xu, and J. A. C. Bland, J. Appl. Phys. **89**, 7018 (2001).
[12] S. W. Sides, P. A. Rikvold, and M. A. Novotny, Phys. Rev. E **59**, 2710 (1999).
[13] B. Raquet, R. Mamy, and J. C. Ousset, Phys. Rev. B **54**, 4128 (1996).
[14] I. F. Lyuksyutov, T. Nattermann, and V. Pokrovsky, Phys. Rev. B **59**, 4260 (1999).
[15] M. Heidkamp and J. L. Erskine, Rev. Sci. Instrum. **71**, 3141 (2000).
[16] H. J. Williams, W. Shockley, and C. Kittel, Phys. Rev. **80**, 1090 (1950).
[17] I. Ruiz-Feal, T. A. Moore, L. Lopez-Diaz, and J. A. C. Bland, Phys. Rev. B **65**, 054409 (2002).
[18] G. Durin and S. Zapperi, cond-mat/0404512 (unpublished).
[19] S. Yang and J. L. Erskine (unpublished).
[20] B. Alessandro, C. Beatrice, G. Bertotti, and A. Montorsi, J. Appl. Phys. **68**, 2901 (1990).
[21] B. Alessandro, C. Beatrice, G. Bertotti, and A. Montorsi, J. Appl. Phys. **68**, 2908 (1990).
[22] G. Bertotti, G. Durin, and A. Magni, J. Appl. Phys. **75**, 5490 (1994).
[23] A. Magni, C. Beatrice, G. Durin, and G. Bertotti, J. Appl. Phys. **86**, 3253 (1999).
[24] S. Zapperi, P. Cizeau, G. Durin and H. E. Stanley, Phys. Rev. B **58**, 6353 (1998).
[25] G. A. Grimes, P. L. Trouilloud, J. K. Lumpp, and G. C. Bush, J. Appl. Phys. **81**, 4720 (1997).
[26] H. Suhl, IEEE Trans. Magn. **34**, 1834 (1998).